Lawrence Berkeley National Laboratory

Title

Doubly Interpenetrated Metal—Organic Framework of pcu Topology for Selective Separation of Propylene from Propane

Permalink

https://escholarship.org/uc/item/0492z04h

Journal

ISSN

Authors

Liu, Ting
Cui, Hui
Zhang, Xin
et al.

Publication Date

DOI

Peer reviewed

A Doubly Interpenetrated Metal-Organic Framework of pcu Topology for Selective Separation of Propylene from Propane

Ting Liu,[a,b] Hui Cui,[b] Xin Zhang,[b,*] Zhi-Yin Zhang,[a] Rui-Biao Lin,[b] Bin Liang,[b] Jian Zhang,[c] Dan Li,[a,*] and Banglin Chen,[b,*]

[a]College of Chemistry and Materials Science, and Guangdong Provincial Key Laboratory of Functional Supramolecular Coordination Materials and Applications, Jinan University, Guangzhou 510632, P. R. China.

[b]Department of Chemistry, University of Texas at San Antonio, One UTSA Circle, San Antonio, Texas 78249-0698, United States.

[c]The Molecular Foundry Lawrence Berkeley National Laboratory Berkeley, Berkeley, CA 94720, United States.

1

ABSTRACT

Adsorptive separation is an appealing alternative technology to reduce the high energy and capital cost of distillation separation of propylene/propane; however, very challenging to realize. A new flexible MOF material [Zn$_2$(BDC-Cl)$_2$(Py$_2$TTz)] with doubly interpenetrated pillared paddle wheel structure of pcu (primitive cubic) topology has been realized for this difficult separation for the first time. Through judicious choice of linkers, the framework has small pore apertures that takes up much more propylene adsorption than propane. The selective adsorption relies on the sieving effect of the flexible framework. Column breakthrough experiment further demonstrated that the efficient separation can be achieved under dynamic conditions.

INTRODUCTION

Propylene is an important chemical feedstock to produce polypropylene which is thermoplastic polymer widely used as film, packaging, and containers due to its high mechanical strength and chemical stability.[1] The production of propylene is the second largest chemical process and the global annual production has reached 114 million metric tons in 2015. During the production of propylene by steam cracking, propane always coexists and need to be removed to yield high purity (> 99.5%) propylene that is suitable for polymer production.[2] The propylene/propane separation is more challenging than ethylene/ethane separation due to the smaller difference of boiling point (5K for propylene/propane vs 15 K for ethylene/ethane). Such separation is usually achieved by multiple distillation-compression cycles in a C3 splitter, which is considered as most energy-intensive distillation process.[3-4] To reduce the energy and capital cost of this challenging

2

separation, researchers have sought for alternative approaches such as membrane separation and adsorption based separation.[5-7]

As an emerging type of crystalline porous material, metal-organic frameworks (MOFs)[8] have demonstrated great potential in a variety of applications[9-13] including gas storage[14-16] and separation[17-25]. The tunable pore sizes and surface functionalities of MOFs allowed rational design for targeted separations. Propylene/propane separation has been explored using MOFs based on kinetic separation or π-complexation mechanism.[26-28] Ultramicroporous MOFs with high sieving effect for propylene over propane produce propylene in high purity, but very challenging to realize,[29-30] due to the requirement of high framework rigidity and proper pore aperture in between the size of the two molecules.[31-32] It is of great significance to develop new materials or mechanisms for this challenging separation.

Pillared paddle wheel frameworks are interesting and classical type of MOFs constructed by connecting 2D layered square lattice network with pillared ligand to form a primitive cubic structure (**pcu** topology).[33-35] The pore size and surface functionality can be tuned by dicarboxylic linker in the 2D network and the pillar pyridyl linker. When long pillar linkers are used, the frameworks prone to form interpenetrated structures, which offered another way to tune the pore sizes. We have demonstrated successful gas chromatography separation of light hydrocarbons with an interpenetrated framework MOF-508 in 2006.[36] Dynamic behavior upon guest exchange or solvent removal was also discovered for the pillared paddle wheel frameworks.[37-38] Recently, the flexibility of this classical type of materials has been studied by tuning pillar linker or dicarboxylic linker for high pressure gas storage and molecular recognition.[39-40] The flexible nature of these pyridyl-carboxylate MOFs have been rarely utilized

for separation, only a few flexible MOFs are being developed for some gas separations, including C_2H_2/CO_2, C_3H_4/C_3H_6 and CO_2 capture from CH_4 and N_2.[41-49] This type of MOFs haven't been yet realized for the challenging propylene/propane separation.

Herein, we report a doubly interpenetrated pillared paddle wheel MOF [Zn_2(BDC-Cl)$_2$(Py$_2$TTz), also denoted as **1**, (BDC-Cl = 2-chloro-terephthalate, Py$_2$TTz = 2,5-bis(4-pyridyl) thiazolo-[5,4-*d*] thiazole)] constructed with a dicarboxylic linker and a dipyridyl pillar linker possessing moderate pore volume while small pore aperture. At 273 K, this material can adsorb large amount of the smaller propylene molecule (74.4 cm^3/g) through gate-opening adsorption, while only small amount of propane (36.2 cm^3/g). The efficient separation was further confirmed by dynamic breakthrough experiment. Our results suggested that the tunable pore aperture of flexible pillared paddle wheel MOF would bring great promise for the challenging hydrocarbon separations such as propylene/propane separation.
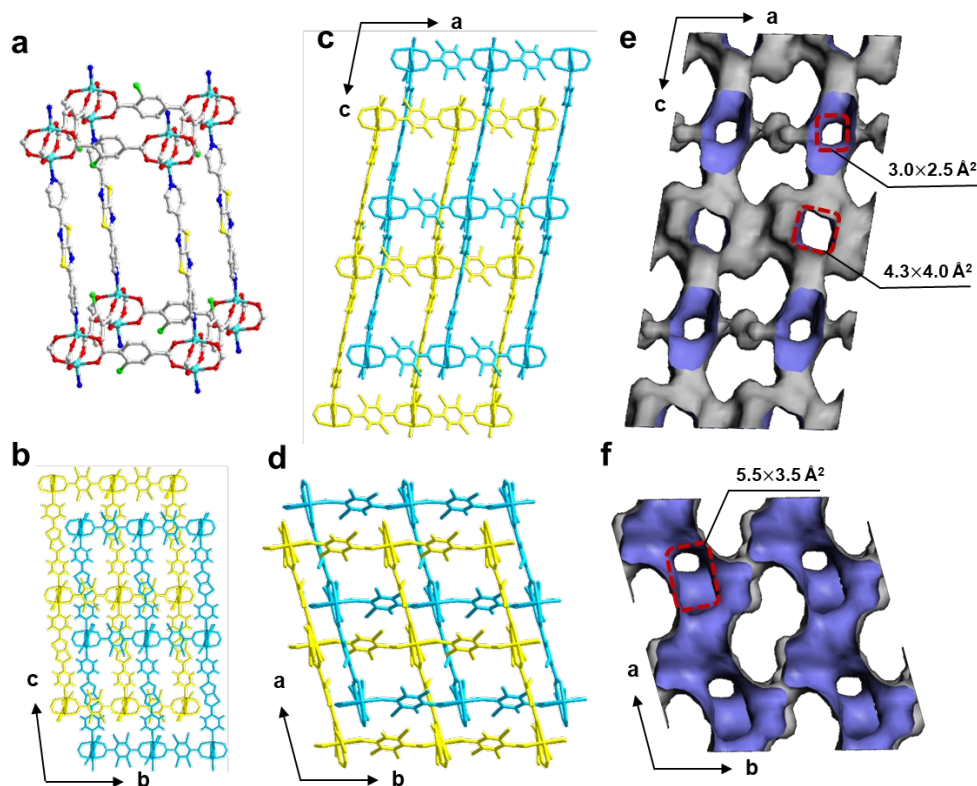
Figure 1. Crystal structure and channels of **1**. a) Basic unit of the **pcu** framework containing Zn paddle wheel, Py$_2$TTz and BDC-Cl ligands; b-d) Interpenetrated framework viewed along *a, b, c* axis respectively; e) Channels and pore apertures along *b* axis; f) Zig-zag channel and pore aperture along *c* axis.

RESULTS AND DISCUSSION

The yellow needle-shaped crystals of **1** were obtained by solvothermal reaction of Zn(NO$_3$)$_2$·6H$_2$O with Py$_2$TTz and 2-chloro-terephthalic acid (2-Cl-H$_2$BDC) in mixed solution of N,N-Dimethylformamide (DMF) and ethanol (v/v=13/1) at 80 °C for 18h (Supporting Information Figure S1). Single-crystal X-ray diffraction analysis reveals that **1** crystallizes in triclinic *P*-1 space group. In the asymmetric unit, there are two Zn (II) atoms, two BDC-Cl

ligands and one Py_2TTz ligand (Figure S2). Each binuclear Zn_2 paddlewheel secondary building unit (SBU) is linked by four carboxylic groups from four distinct BDC-Cl dicarboxylate linker to form a 2D layer with square lattice network in the *ab*-plane. These layered square lattice nets are further pillared by Py_2TTz linkers through occupying the axial sites of Zn_2 paddle wheels along the *c* axis, generating a three-dimensional (3D) elongated primitive cubic (**pcu**) network (Figure 1a-d). Two independent sets of **pcu** networks are interpenetrated, forming a framework with interconnected channels on *bc*-plane. The combination of short dicarboxylic linker and long bipyridine linker enabled relatively large cage size and small aperture size. Zig-zag type of channel can be found along crystallographic *b* and *c* axis with two types of aperture of 4.3×4.0 $Å^2$ and 3.0×2.5 $Å^2$ along the *b* axis (Figure 1e) and another aperture of 5.5×3.5 $Å^2$ along *c* axis (Figure 1f). These pore apertures are slightly smaller than the kinetic diameter of propylene (4.68 Å) and propane (5.1 Å). Since this type of frameworks often exhibit flexibility, the pore aperture may slightly expand to accommodate propylene while still exclude propane. The bulk phase purity was confirmed by powder x-ray diffraction (PXRD), as shown in Figure S3. Upon activation, some peaks of **1a** shifted slightly to lower angle, indicating slight framework expansion and certain flexibility of this material. Thermogravimetric analysis revealed that both **1** and **1a** are thermally stable up to ~ 350 °C (Figure S4).
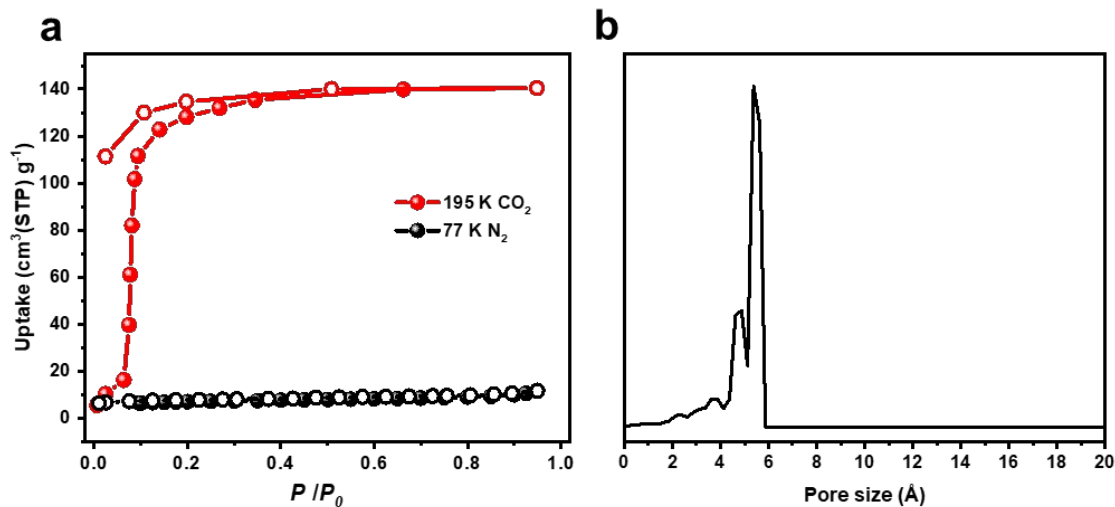
Figure 2. Porosity establishment of **1a**. a) Adsorption isotherm of CO_2 at 195 K and N_2 at 77 K; b) Pore size distribution calculated based on crystal structure.

The porosity of activated **1a** was examined by N_2 (77K) and CO_2 (195K) adsorption measurement (Figure 2a). Prior to analysis, the ethanol exchanged sample was activated under vacuum at room temperature for nine hours. Significant amount of CO_2 (140 cm^3/g) was adsorbed by **1a** at 195K and a typical gate-opening process occurred at ~ 48 mmHg (0.063 P/P_0) showing a type F-II isotherm with a small hysteresis.[50] Such adsorption behavior indicates that the framework has certain flexibility and may involve a structural transformation or pore aperture expansion during the adsorption process. Based on the CO_2 adsorption isotherm at 195 K, the BET surface area and pore volume of **1a** was determined to be 441 m^2/g and 0.257 cm^3/g. The measured pore volume is very close to the theoretical pore volume (0.287 cm^3/g) based on the crystal structure. In contrast, there is no appreciable adsorption observed in N_2 isotherm, probably because N_2 exhibit larger kinetic diameter and weaker interfacial interactions with the framework than those of CO_2 and could not induce the structural transition. The pore size of **1**

was calculated by Poreblazer program[51] based on the crystal structure. As shown in Figure 2b, two major pore sizes of 5.4 Å and 4.9 Å can be found in the structure. The pore size is comparable to the kinetic diameter of propylene (4.68 Å), which may lead to efficient confinement of propylene molecule.
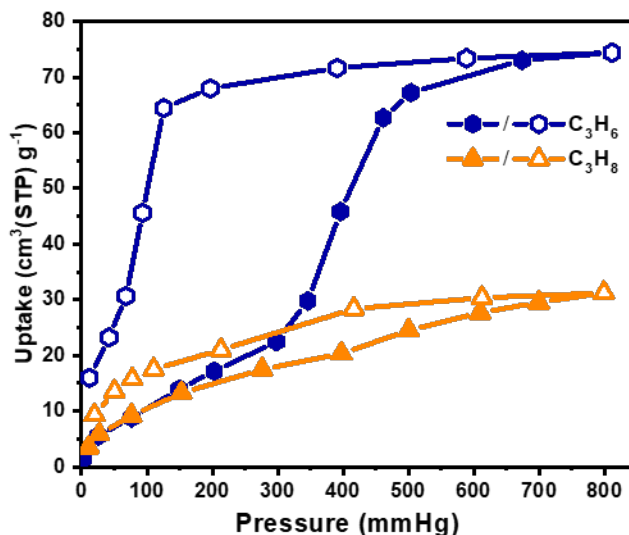
Figure 3. C_3H_6 and C_3H_8 adsorption (solid symbol) and desorption (hollow symbol) isotherms at 273 K.

The flexible nature of **1a** promoted us to evaluate the separation performance of propylene and propane. Single component adsorption isotherms of C_3H_6 and C_3H_8 were measured at 273K (Figure 3). The C_3H_6 adsorption increased abruptly at ~ 300 mmHg and adsorption amount increased from 22.5 to 74.4 cm^3/g (800 mmHg). Such adsorption curve is typical for flexible MOFs, indicating the dynamic structure can expand the small pore aperture to adsorb extra C_3H_6 molecules. In contrast, C_3H_8 adsorption is typical type I isotherm and the total adsorption (36.2 cm^3/g) is much smaller than that of C_3H_6. The different adsorption behavior of C_3H_8 is likely because the molecular size is too large to enter through the small pore aperture.

The larger C_3H_8 molecule also requires higher degree of pore aperture expansion, therefore the gate-opening process less likely occur and the C_3H_8 adsorption curve is similar to those of rigid MOFs. Overall, the C_3H_6 adsorption capacity is 106% higher than C_3H_8 adsorption capacity at 273 K, indicating the promising separation of C_3H_6 and C_3H_8. For the quantitative evaluation on potential separation performance of C_3H_6/C_3H_8 at 273 K using **1**a, the uptake ratio of C_3H_6/C_3H_8 was calculated as ~ 2.3 and 2.1 under 0.6 bar and 1 bar respectively. At 298K, **1a** adsorbs small amount of C_3H_8 (22.6 cm^3/g) and C_3H_6 (31.2 cm^3/g) at 800 mmHg (Figure S5). The heat of adsorption (Q_{st}) of C_3H_6 and C_3H_8 were calculated based on adsorption isotherms at 273 K and 298 K. The Q_{st} of C_3H_6 is slightly smaller than that of C_3H_8, probably because part of the heat of adsorption is compensated to the energy required for structural change (Figure S6). The higher Q_{st} at higher loading may also associated with stronger guest-guest interactions.
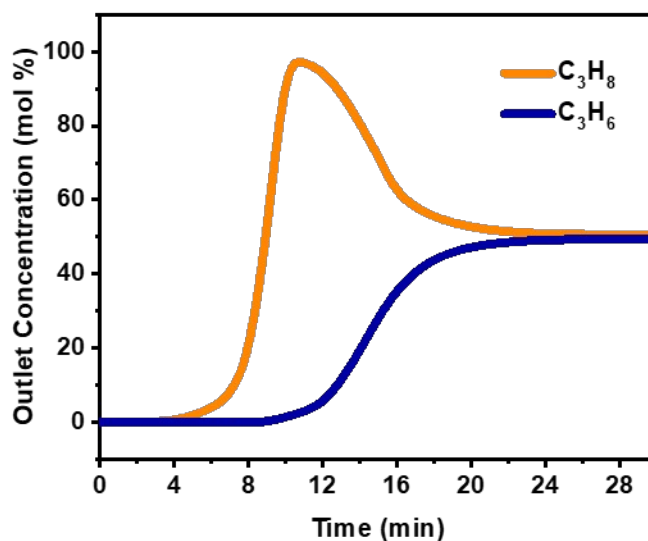
Figure 4. Column breakthrough curve of **1a** using equal molar C_3H_6 and C_3H_8, flow rate of 2 ml/min under 1.2 bar and 273 K.

To simulate the practical separation of C_3H_6/C_3H_8, the breakthrough experiment was carried out. Equimolar C_3H_6/C_3H_8 gas mixture was passed through a packed column of activated **1a** sample with a total flow of 2 mL/min at 273 K and 1.2 bar. The partial pressure of each component is 0.6 bar which corresponds to the high C_3H_6/C_3H_8 uptake ratio of ~ 2.3. As shown in Figure 4, C_3H_8 first broke through the packed column after 4 min because of its smaller uptake capacity in **1a**, while C_3H_6 started to break through after 9 min and saturated at 22 min. For a given cycle, the captured gas amount under dynamic conditions was 1.42 mmol/g for C_3H_6 and 0.27 mmol/g for C_3H_8 with the C_3H_6/C_3H_8 selectivity up to 5.2. Such results demonstrated that efficient separation of C_3H_6/C_3H_8 mixture under dynamic condition can be achieved with the flexible framework **1a**.

CONCLUSIONS

In summary, we realized efficient C_3H_6/C_3H_8 separation by a flexible MOF material with interpenetrated pillared paddle wheel structure. The small pore aperture and this flexible MOF enabled propylene adsorption through gate-opening process, while only limited amount of the larger propane molecule can be adsorbed. Overall, adsorption capacity of C_3H_6 is ~106% higher than that of C_3H_8 at 273 K. Column breakthrough experiment demonstrated the efficient separation of an equal molar C_3H_6/C_3H_8 mixture under dynamic conditions. Such results illustrated that flexible carboxylate-pyridyl frameworks with small pore apertures are promising candidates for the very challenging gas separations. It is foreseeable that the separation concept of this work would be widely adopted for broad range of important separations in the near future.

EXPERIMENTAL SECTION

Materials and Methods. All general reagents and solvents (AR grade) were commercially available and used directly as received. The ligands of 2,5-bis(4-pyridyl) thiazolo-[5,4-*d*] thiazole (Py$_2$TTz)[52] and 2-chloro-terephthalic acid (2-Cl-H$_2$BDC)[53] were prepared according to the reported protocols and described in detail in Supporting Information. Powder X-ray diffraction (PXRD) data were collected on a Rigaku Smartlab3 X-ray powder diffractometer equipped with a Cu sealed tube (λ = 1.54178 Å) at room temperature. Thermogravimetric analyses (TGA) were performed under nitrogen atmosphere with a heating rate of 10 °C/min on TGA-50 (SHIMADZU) thermogravimetric analyzer. Adsorption isotherms of N$_2$, CO$_2$, C$_3$H$_6$, and C$_3$H$_8$ were collected on a Micromeritics ASAP 2020 surface area analyzer.

Synthesis of 1 Crystals of **1** were prepared through solvothermal reaction conditions used for pillared paddle wheel architectures. A mixture of Zn(NO$_3$)$_2$·6H$_2$O (12 mg, 0.040 mmol), Py$_2$TTz(6 mg, 0.020 mmol), 2-Cl-H$_2$BDC (8.02 mg, 0.04 mmol) were added to a 7mL solution of DMF and EtOH (v/v=13/1) in a screw capped vial. Then the reaction mixture was put in an oven and heated at 80 °C for 18 h to obtain crystals suitable for single-crystal X-ray diffraction (SXRD) analysis. The resultant yellow colored crystals were collected and washed with DMF and EtOH and dried under vaccum (yield: 65% based on the organic ligand). Elemental analysis of **1**·DMF (formula: C$_{33}$H$_{21}$N$_5$S$_2$O$_9$Cl$_2$Zn$_2$): calcd. C 44.17 %, H 2.53 %, N 8.12 %; found C 44.17 %, H 2.35 %, N 7.80 %.

Crystallography Analysis. The crystallographic data of **1** were collected on a Rigaku supernova X-ray diffractometer with graphite monochromatic Cu Kα radiation (λ = 1.54184 Å) at room temperature. The structure was solved by direct methods first and refined further with ShelXL refinement package using full-matrix least-squares on F^2 with anisotropic displacement. Non-hydrogen atoms were refined with anisotropic displacement parameters in the final cycles. All hydrogen atoms were calculated in idealized positions with isotropic displacement parameters. The detailed structural refinements can be found in Table S1 in the Supporting Information. The supplementary crystallographic data for **1** (CCDC number : 2016038) can be found free of charge from the Cambridge Crystallographic Data Center via www.ccdc.cam.ac.uk/data_request/ cif.

Breakthrough Experiments. The breakthrough experiments were carried out on a home-made dynamic gas breakthrough instrument with a gas mixture of C_3H_6/C_3H_8 (50/50 v/v) at 273K. The gas flow and pressure were controlled and monitored by a mass flow controller and a pressure controller valve. Outlet composition was monitored periodically by using a gas chromatography (GC-2014, SHIMADZU) with a thermal conductivity detector (TCD). The microcrystalline sample of **1** (0.55 g) was firstly packed into a stainless-steel column with inner dimensions of ϕ = 4 × 150 mm and then was purged with He gas flow (30 mL/min) overnight at room temperature. The mixed gas flow rate during breakthrough process is 2 mL/min at 1.2 bar. After the breakthrough experiment, the adsorbent was regenerated by a He flow (40 mL/min) at room temperature until no detectable C_3H_6 and C_3H_8 were found.

ASSOCIATED CONTENT

Supporting Information

The Supporting Information is available free of charge at

https://pubs.acs.org/doi/xxxxx/acsami.xxxxx.

Synthesis of ligands, crystallographic table, and supplemental figures of PXRD, TG, adsorption isotherm and Q_{st} (PDF)

Crystallographic information file (CCDC No. 2016038 (**1**)) (CIF)

AUTHOR INFORMATION

Corresponding Author

Xin Zhang (email: xin.zhang2@utsa.edu), Dan Li (email: danli@jnu.edu.cn), and Banglin Chen (email: banglin.chen@utsa.edu).

Notes

The authors declare no competing financial interest.

REFERENCES

(1) Whiteley, K.S. (2011). Polyethylene. In *Ullmann's Encyclopedia of Industrial Chemistry*; pp 1-42.

(2) Christopher, C. C. E.; Dutta, A.; Farooq, S.; Karimi, I. A. Process Synthesis and Optimization of Propylene/Propane Separation Using Vapor Recompression and Self-Heat Recuperation. *Ind. Eng. Chem. Res.* **2017,** *56*, 14557-14564.

(3) Sholl, D. S.; Lively, R. P. Seven Chemical Separations to Change the World. *Nature* **2016,** *532*, 435-437.

(4) Jarvelin, H.; Fair, J. R. Adsorptive Separation of Propylene-propane Mixtures. *Ind. Eng. Chem. Res.* **1993,** *32*, 2201-2207.

(5) Liu, Y.; Chen, Z.; Liu, G.; Belmabkhout, Y.; Adil, K.; Eddaoudi, M.; Koros, W. Conformation-Controlled Molecular Sieving Effects for Membrane-Based Propylene/Propane Separation. *Adv. Mater.* **2019,** *31*, 1807513.

(6) Zhang, C.; Zhang, K.; Xu, L.; Labreche, Y.; Kraftschik, B.; Koros, W. J. Highly Scalable ZIF-based Mixed-matrix Hollow Fiber Membranes for Advanced Hydrocarbon Separations. *AlChE J.* **2014,** *60*, 2625-2635.

(7) Olson, D. H.; Camblor, M. A.; Villaescusa, L. A.; Kuehl, G. H. Light Hydrocarbon Sorption Properties of Pure Silica Si-CHA and ITQ-3 and High Silica ZSM-58. *Microporous Mesoporous Mater.* **2004,** *67*, 27-33.

(8) Furukawa, H.; Cordova, K. E.; O'Keeffe, M.; Yaghi, O. M. The Chemistry and Applications of Metal-Organic Frameworks. *Science* **2013,** *341*, 1230444.

(9) Islamoglu, T.; Chen, Z.; Wasson, M. C.; Buru, C. T.; Kirlikovali, K. O.; Afrin, U.; Mian, M. R.; Farha, O. K. Metal-Organic Frameworks against Toxic Chemicals. *Chem. Rev.* **2020**, DOI: 10.1021/acs.chemrev.9b00828.

(10) Drout, R. J.; Robison, L.; Farha, O. K. Catalytic Applications of Enzymes Encapsulated in Metal–Organic Frameworks. *Coord. Chem. Rev.* **2019,** *381*, 151-160.

(11) Jiao, L.; Jiang, H.-L. Metal-Organic-Framework-Based Single-Atom Catalysts for Energy Applications. *Chem* **2019,** *5*, 786-804.

(12) Zhang, X.; Wang, B.; Alsalme, A.; Xiang, S.; Zhang, Z.; Chen, B. Design and Applications of Water-Stable Metal-Organic Frameworks: Status and Challenges. *Coord. Chem. Rev.* **2020,** *423*, 213507.

(13) Wang, P.-L.; Xie, L.-H.; Joseph, E. A.; Li, J.-R.; Su, X.-O.; Zhou, H.-C. Metal–Organic Frameworks for Food Safety. *Chem. Rev.* **2019,** *119*, 10638-10690.

(14) Li, H.; Li, L.; Lin, R.-B.; Zhou, W.; Zhang, Z.; Xiang, S.; Chen, B. Porous Metal-Organic Frameworks for Gas Storage and Separation: Status and Challenges. *EnergyChem* **2019,** *1*, 100006.

(15) Chen, Z.; Li, P.; Anderson, R.; Wang, X.; Zhang, X.; Robison, L.; Redfern, L. R.; Moribe, S.; Islamoglu, T.; Gomez-Gualdron, D. A.; Yildirim, T.; Stoddart, J. F.; Farha, O. K. Balancing Volumetric and Gravimetric Uptake in Highly Porous Materials for Clean Energy. *Science* **2020,** *368*, 297-303.

(16) Zhang, X.; Lin, R.-B.; Wang, J.; Wang, B.; Liang, B.; Yildirim, T.; Zhang, J.; Zhou, W.; Chen, B. Optimization of the Pore Structures of MOFs for Record High Hydrogen Volumetric Working Capacity. *Adv. Mater.* **2020,** *32*, 1907995.

(17) Lin, R.-B.; Xiang, S.; Zhou, W.; Chen, B. Microporous Metal-Organic Framework Materials for Gas Separation. *Chem* **2020**, *6*, 337-363.

(18) Yang, L.; Qian, S.; Wang, X.; Cui, X.; Chen, B.; Xing, H. Energy-efficient Separation Alternatives: Metal-Organic Frameworks and Membranes for Hydrocarbon Separation. *Chem. Soc. Rev.* **2020,** *49*, 5359-5406.

(19) Barnett, B. R.; Gonzalez, M. I.; Long, J. R. Recent Progress Towards Light Hydrocarbon Separations Using Metal–Organic Frameworks. *Trends in Chemistry* **2019,** *1*, 159-171.

(20) Adil, K.; Belmabkhout, Y.; Pillai, R. S.; Cadiau, A.; Bhatt, P. M.; Assen, A. H.; Maurin, G.; Eddaoudi, M. Gas/vapour Separation using Ultra-microporous Metal-Organic Frameworks: Insights into the Structure/separation Relationship. *Chem. Soc. Rev.* **2017,** *46*, 3402-3430.

(21) Liao, P.-Q.; Huang, N.-Y.; Zhang, W.-X.; Zhang, J.-P.; Chen, X.-M. Controlling Guest Conformation for Efficient Purification of Butadiene. *Science* **2017,** *356*, 1193-1196.

(22) Huang, Y.-L.; Qiu, P.-L.; Zeng, H.; Liu, H.; Luo, D.; Li, Y. Y.; Lu, W.; Li, D. Tuning the C2/C1 Hydrocarbon Separation Performance in a BioMOF by Surface Functionalization. *Eur. J. Inorg. Chem.* **2019,** *2019*, 4205-4210.

(23) Zeng, H.; Xie, X. J.; Xie, M.; Huang, Y. L.; Luo, D.; Wang, T.; Zhao, Y.; Lu, W.; Li, D. Cage-Interconnected Metal-Organic Framework with Tailored Apertures for Efficient C_2H_6/C_2H_4 Separation under Humid Conditions. *J. Am. Chem. Soc.* **2019,** *141*, 20390-20396.

(24) Li, B.; Wen, H.-M.; Yua, Y.; Cui, Y.; Zhou, W.; Chen, B.; Qian, G. Nanospace within Metal–Organic Frameworks for Gas Storage and Separation. *Mater. Today Nano*, **2018**, *2*, 21-49.

(25) Pei, J.; Shao, K.; Wang, J.-X.; Wen, H.-M.; Yang, Y.; Cui, Y.; Krishna, R.; Li, B.; Qian. G. A Chemically Stable Hofmann-Type Metal−Organic Framework with Sandwich-Like Binding Sites for Benchmark Acetylene Capture. *Adv. Mater.* **2020**, *32*, 1908275.

(26) Wang, Y.; Huang, N.-Y.; Zhang, X.-W.; He, H.; Huang, R.-K.; Ye, Z.-M.; Li, Y.; Zhou, D.-D.; Liao, P.-Q.; Chen, X.-M.; Zhang, J.-P. Selective Aerobic Oxidation of a Metal-Organic Framework Boosts Thermodynamic and Kinetic Propylene/Propane Selectivity. *Angew. Chem. Int. Ed.* **2019,** *58*, 7692-7696.

(27) Li, L.; Lin, R.-B.; Wang, X.; Zhou, W.; Jia, L.; Li, J.; Chen, B. Kinetic Separation of Propylene over Propane in a Microporous Metal-Organic Framework. *Chem. Eng. J.* **2018,** *354*, 977-982.

(28) Bloch, E. D.; Queen, W. L.; Krishna, R.; Zadrozny, J. M.; Brown, C. M.; Long, J. R. Hydrocarbon Separations in a Metal-Organic Framework with Open Iron(II) Coordination Sites. *Science* **2012,** *335*, 1606-1610.

(29) Yang, L.; Cui, X.; Yang, Q.; Qian, S.; Wu, H.; Bao, Z.; Zhang, Z.; Ren, Q.; Zhou, W.; Chen, B.; Xing, H. A Single-Molecule Propyne Trap: Highly Efficient Removal of Propyne from Propylene with Anion-Pillared Ultramicroporous Materials. *Adv. Mater.* **2018,** *30*, 1705374.

(30) Cadiau, A.; Adil, K.; Bhatt, P. M.; Belmabkhout, Y.; Eddaoudi, M. A Metal-Organic Framework-based Splitter for Separating Propylene from Propane. *Science* **2016,** *353*, 137-40.

(31) Li, B.; Cui, X.; O'Nolan, D.; Wen, H.-M.; Jiang, M.; Krishna, R.; Wu, H.; Lin, R.-B.; Chen, Y.-S.; Yuan, D.; Xing, H.; Zhou, W.; Ren, Q.; Qian, G.; Zaworotko, M. J.; Chen, B. An Ideal Molecular Sieve for Acetylene Removal from Ethylene with Record Selectivity and Productivity. *Adv. Mater.* **2017,** *29*, 1705374.

(32) Lin, R.-B.; Li, L.; Zhou, H.-L.; Wu, H.; He, C.; Li, S.; Krishna, R.; Li, J.; Zhou, W.; Chen, B. Molecular Sieving of Ethylene from Ethane using a Rigid Metal-Organic Framework. *Nat. Mater.* **2018,** *17*, 1128-1133.

(33) Chun, H.; Dybtsev, D. N.; Kim, H.; Kim, K. Synthesis, X-ray Crystal Structures, and Gas Sorption Properties of Pillared Square Grid Nets based on Paddle-wheel Motifs: Implications for Hydrogen Storage in Porous Materials. *Chem. Eur. J.* **2005,** *11*, 3521-3529.

(34) Ma, B.-Q.; Mulfort, K. L.; Hupp, J. T. Microporous Pillared Paddle-wheel Frameworks based on Mixed-ligand Coordination of Zinc Ions. *Inorg. Chem.* **2005,** *44*, 4912-4914.

(35) Seki, K.; Mori, W. Syntheses and Characterization of Microporous Coordination Polymers with Open Frameworks. *J. Phys. Chem. B* **2002,** *106*, 1380-1385.

(36) Chen, B.; Liang, C.; Yang, J.; Contreras, D. S.; Clancy, Y. L.; Lobkovsky, E. B.; Yaghi, O. M.; Dai, S. A Microporous Metal-Organic Framework for Gas-Chromatographic Separation of Alkanes. *Angew. Chem. Int. Ed.* **2006,** *45*, 1390-1393.

(37) Dybtsev, D. N.; Chun, H.; Kim, K. Rigid and Flexible: A Highly Porous Metal–Organic Framework with Unusual Guest-Dependent Dynamic Behavior. *Angew. Chem. Int. Ed.* **2004,** *116*, 5143-5146.

(38) Chen, B.; Ma, S.; Zapata, F.; Lobkovsky, E. B.; Yang, J. Hydrogen Adsorption in an Interpenetrated Dynamic Metal-Organic Framework. *Inorg. Chem.* **2006,** *45*, 5718-5720.

(39) Zhu, A.-X.; Yang, Q.-Y.; Mukherjee, S.; Kumar, A.; Deng, C.-H.; Bezrukov, A. A.; Shivanna, M.; Zaworotko, M. J. Tuning the Gate-Opening Pressure in a Switching pcu Coordination Network, X-pcu-5-Zn, by Pillar-Ligand Substitution. *Angew. Chem. Int. Ed.* **2019,** *58*, 18212-18217.

(40) Gu, Y.; Zheng, J.-J.; Otake, K. I.; Sugimoto, K.; Hosono, N.; Sakaki, S.; Li, F.; Kitagawa, S. Structural-Deformation-Energy-Modulation Strategy in a Soft Porous Coordination Polymer with an Interpenetrated Framework. *Angew. Chem. Int. Ed.* **2020**, DOI: 10.1002/anie.202003186.

(41) Kitaura, R.; Seki, K.; Akiyama, G.; Kitagawa, S. Porous Coordination-polymer Crystals with Gated Channels Specific for Supercritical Gases. *Angew. Chem. Int. Ed.* **2003,** *42*, 428-431.

(42) Zeng, H.; Xie, M.; Huang, Y.-L.; Zhao, Y.; Xie, X.-J.; Bai, J.-P.; Wan, M.-Y.; Krishna, R.; Lu, W.; Li, D. Induced Fit of C_2H_2 in a Flexible MOF Through Cooperative Action of Open Metal Sites. *Angew. Chem. Int. Ed.* **2019,** *58*, 8515-8519.

(43) Li, L.; Lin, R.-B.; Krishna, R.; Wang, X.; Li, B.; Wu, H.; Li, J.; Zhou, W.; Chen, B. Flexible-Robust Metal-Organic Framework for Efficient Removal of Propyne from Propylene. *J. Am. Chem. Soc.* **2017,** *139*, 7733-7736.

(44) Wang, H.; Dong, X.; Velasco, E.; Olson, D. H.; Han, Y.; Li, J. One-of-a-kind: a Microporous Metal–Organic Framework Capable of Adsorptive Separation of Linear, Mono- and Di-branched Alkane Isomers via Temperature- and Adsorbate-dependent Molecular Sieving. *Energy Environ. Sci.* **2018,** *11*, 1226-1231.

(45) Zhang, J.-P.; Zhou, H.-L.; Zhou, D.-D.; Liao, P.-Q.; Chen, X.-M. Controlling Flexibility of Metal–Organic Frameworks. *Nati. Sci. Rev.* **2018,** *5*, 907-919.

(46) Evans, J. D.; Bon, V.; Senkovska, I.; Lee, H. C.; Kaskel, S. Four-dimensional Metal-Organic Frameworks. *Nat. Commun.* **2020,** *11*, 2690.

(47) Chen, Y.; Qiao, Z.; Lv, D.; Duan, C.; Sun, X.; Wu, H.; Shi, R.; Xia, Q.; Li, Z. Efficient Adsorptive Separation of C_3H_6 over C_3H_8 on Flexible and Thermoresponsive CPL-1. *Chem. Eng. J.* **2017,** *328*, 360-367.

(48) Lin, R.-B.; Li, L.; Wu, H.; Arman, H.; Li, B.; Lin, R.-G.; Zhou, W.; Chen, B. Optimized Separation of Acetylene from Carbon Dioxide and Ethylene in a Microporous Material. *J. Am. Chem. Soc.* **2017,** *139*, 8022-8028.

(49) Li, B.; Chen, B. A Flexible Metal-Organic Framework with Double Interpenetration for Highly Selective CO_2 Capture at Room Temperature. *Sci. China Chem.* **2016,** *59*, 965-969.

(50) Yang, Q.-Y.; Lama, P.; Sen, S.; Lusi, M.; Chen, K.-J.; Gao, W.-Y.; Shivanna, M.; Pham, T.; Hosono, N.; Kusaka, S.; Perry, J. J. t.; Ma, S.; Space, B.; Barbour, L. J.; Kitagawa, S.; Zaworotko, M. J. Reversible Switching between Highly Porous and Nonporous Phases of an Interpenetrated Diamondoid Coordination Network That Exhibits Gate-Opening at Methane Storage Pressures. *Angew. Chem. Int. Ed.* **2018,** *57*, 5684-5689.

(51) Sarkisov, L.; Harrison, A. Computational Structure Characterisation Tools in Application to Ordered and Disordered Porous Materials. *Mol. Simulat.* **2011,** *37*, 1248-1257.

(52) Hisamatsu, S.; Masu, H.; Azumaya, I.; Takahashi, M.; Kishikawa, K.; Kohmoto, S. U-Shaped Aromatic Ureadicarboxylic Acids as Versatile Building Blocks: Construction of Ladder and Zigzag Networks and Channels. *Cryst. Growth Des.* **2011,** *11*, 5387-5395.

(53) Goh, T. W.; Xiao, C.; Maligal-Ganesh, R. V.; Li, X.; Huang, W. Utilizing Mixed-linker Zirconium based Metal-Organic Frameworks to Enhance the Visible Light Photocatalytic Oxidation of Alcohol. *Chem. Eng. Sci.* **2015,** *124*, 45-51.
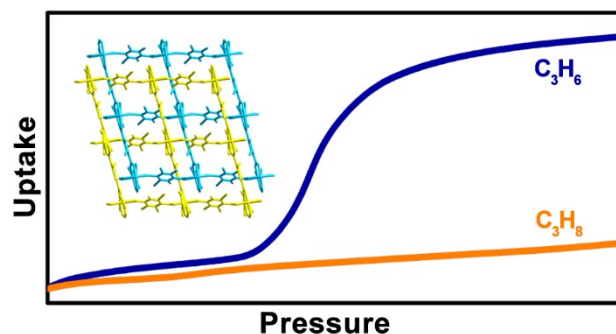
For Table of Contents Only